

# Prediction of Bread Crumb Density by Digital Image Analysis

M. C. Zghal,<sup>1</sup> M.G. Scanlon,<sup>1,2</sup> and H. D. Sapirstein<sup>1</sup>

## ABSTRACT

Cereal Chem. 76(5):734–742

The cellular structure of bread crumb (crumb grain) is an important factor that contributes to the textural properties of fresh bread. The accuracy of a digital image analysis (DIA) system for crumb grain measurement was evaluated based on its capability to predict bread crumb density from directly computed structural parameters. Bread was prepared from representative flour samples of two different wheat classes, Canada Western Red Spring (CWRS) and Canada Prairie Spring (CPS). Dough mixing and proofing conditions were varied to manipulate loaf volume and crumb density. Sliced bread was subjected to DIA immediately after physical density measurement. Experiments were repeated for the same bread samples after drying to three different moisture contents. Five computed crumb grain

parameters were assessed: crumb brightness, cell wall thickness (CWT), void fraction (VF), mean cell area, and crumb fineness (measured as number of cells/cm<sup>2</sup>). Crumb density ranged from 0.088 to 0.252 g/cm<sup>3</sup> depending on proofing and mixing treatments, and was predominantly affected by the former. With increasing crumb density, bread crumb became brighter in appearance, mean cell size and CWT decreased, crumb fineness increased, and the VF decreased. Approximately 80% of the variation in fresh or dried crumb density could be predicted using a linear regression model with two variables, CWT and VF. Results indicated that DIA of directly computed crumb grain could accurately predict bread crumb density after images had been correctly classified into cells and background.

Analysis of product appearance by digital image processing has been shown to be a very effective and reliable method for inspecting and grading food and agricultural products (Chan and Batchelor 1993, Gunasekaran and Ding 1994, Tao et al 1995, Gerrard et al 1996). In the cereals industry, it has been applied in widely different ways for objective assessment of the quality of the crumb grain of bread or cake (Bertrand et al 1992; Sapirstein et al 1992, 1994; Wang and Coles 1993, 1994; Zayas 1993; Rogers et al 1995; Sapirstein 1995, 1999; Zayas et al 1995).

In addition to crumb grain appearance, physical texture is also an important quality factor for baked products. Kamman (1970) concluded that texture of bread crumb is affected by the character of the grain. He speculated that cell wall thickness (CWT), cell size, and uniformity are factors that can influence the texture of bread crumb. This view is supported by materials science which provides strong evidence relating the mechanical properties of cellular materials to their structural characteristics (Gibson and Ashby 1988). Therefore, it is conceivable that digital image analysis (DIA), which can provide an assessment of the structural appearance of the bread crumb, can also be used to estimate the physical texture (or mechanical properties) of this cellular solid.

To establish a relationship between the structural and textural properties in bread crumb, the technique for measuring crumb grain must be accurate and precise. Validating the method for measuring crumb grain is therefore a critical step that must be performed. The objective of this study, which is an extension of previous work (Sapirstein et al 1994, 1999), was to determine the accuracy of the DIA system by means of crumb density prediction based on computed crumb grain features. Density was chosen because it is an important physical property that contributes to the texture of foods of cereal origin possessing a porous structure (Ponte et al 1962, Attenburrow et al 1989, Barrett et al 1994, Bhatnagar and Hanna 1997) and can be easily measured. To generate a range of densities in the bread crumb, various mixing and proofing times were used in the breadmaking procedure.

## MATERIALS AND METHODS

### Flour

Representative samples of sound wheat of two wheat classes, Canada Western Red Spring (CWRS) and Canada Prairie Spring White (CPS), were milled to straight-grade flour on a pilot mill

(Canadian International Grains Institute, Winnipeg, MB). The CWRS and CPS flours contained 13.5 and 10.4% protein (14% mb) and had farinograph absorptions of 65 and 57%, respectively.

### Baking

Bread (100 g, flour basis) was baked using a straight-dough, short-time process (Yamada and Preston 1992) with minor modifications; ascorbic acid was added at a level of 150 ppm. Baking absorption, which was optimized based on the handling properties of the doughs at panning, was 68 and 60% for the CWRS and CPS flours, respectively. Five mixing times and three proofing times were used to obtain a wide range of crumb density. Optimally developed doughs were prepared by mixing 10% past peak dough resistance on a GRL 200 mixer (Hlynka and Anderson 1955, Kilborn and Dempster 1965). This level of mixing is commonly used for the GRL 200 mixer and is considered to be optimal (Kilborn and Tipples 1981, Yamada and Preston 1992). For the CWRS and CPS flours, these dough mixing times were 8.3 and 5.5 min, respectively. Mixing times were chosen so that doughs were under- and overmixed by 20 and 40% of the optimum mixing times. After mixing, doughs were processed as described by Yamada and Preston (1992), proofed, and baked for 30 min at 204°C. The three proofing times were 35, 70, and 105 min. Loaves were allowed to cool for 25 min before loaf volume measurement by rapeseed displacement. Bread loaves were sealed in double bags of 2-mil (51- $\mu$ m) polyethylene (Bel Art, Newark, NJ) and stored overnight at 21°C to allow for moisture equilibration. For each flour, the 15 mixing and proofing time treatments were randomly applied, and breadmaking was replicated three times over a six-week period using a different batch of compressed yeast (Fleischmann's, Calgary, AB) for each replicate.

### Density Measurement

Bread loaves were sliced transversely (12 mm thickness) using a mechanical bread slicer (Oliver model 697, Grand Rapids, MI). After slicing, the bread was rebagged to prevent moisture loss. Five central slices were selected from each loaf. For each slice, one rectangular specimen of crumb was extracted in a central region as previously indicated (Fig. 1, Sapirstein et al 1994). The crumb specimen was carefully excised with a pathology trimming blade cutting around a 60- × 80-mm wooden template; a sawing motion was used to prevent crumb compression. The crumb specimens were kept in covered petri dishes throughout the experiment to reduce moisture loss. The volume of each specimen was determined by taking four measurements along the length (two per slice face), six along the width (three per slice face), and two measurements of thickness using digital callipers (Mitutoyo Corp., Minato-ku, Tokyo). Crumb specimens were weighed just before acquiring digital images.

<sup>1</sup> Dept. Food Science, University of Manitoba, Winnipeg, MB, R3T 2N2, Canada.

<sup>2</sup> Corresponding author: E-mail: scanlon@cc.umanitoba.ca

### Image Analysis

Images of bread slices were acquired using a custom-built digital image analysis (DIA) system described by Sapirstein et al (1994). The monochrome CCD camera was fitted with a 50-mm *f*-1.4 fixed-focus C-mount lens (Fuji-non Inc.) using 11.5 mm of extension. The image segmentation method, based on the *K*-means algorithm, was used for classifying digitized images into cells and background (Sapirstein et al 1994). This algorithm adapts the gray level thresholding of each bread slice image, depending on the overall brightness of the crumb image and the distribution of constituent pixel gray levels, both of which can be affected by the crumb structure itself. Figure 1 (A–D) illustrates the performance of this approach using representative slices of underproofed (Fig. 1A) and overproofed (Fig. 1B) bread. The corresponding segmented images (Fig. 1C and D, respectively) appear to provide an accurate binary representation of the complex cellular structure seen in the original gray-scale images. Aspects related to the accuracy of this

algorithm compared to an alternate approach to image segmentation have been recently reported (Sapirstein 1999).

The uniformity and precision of the imaging system's gray level (GL) response was calibrated using a white opal acrylic plastic working standard (Chemacryl Plastic Ltd., Rexdale, ON) with a nominal reflectance of 81%. The lens aperture was manually adjusted until the computed mean GL corresponded to a target GL value of 160; the latter was predetermined to provide an optimal dynamic range of GL reflectance for bread crumb. GL calibration was then confirmed using three gray levels of a 12-step reflectance calibrated paper gray scale (cat. 152 2267, Kodak, Rochester, NY). The gray level calibration of the imaging system was performed before each imaging session.

Bread slices were examined from a working distance (lens to face of the bread slice) of 27.2 cm. The field of view (FOV) was 45 × 34 mm, with a spatial resolution of ≈70 μm of crumb per pixel length. Digital images of both sides of the crumb specimens

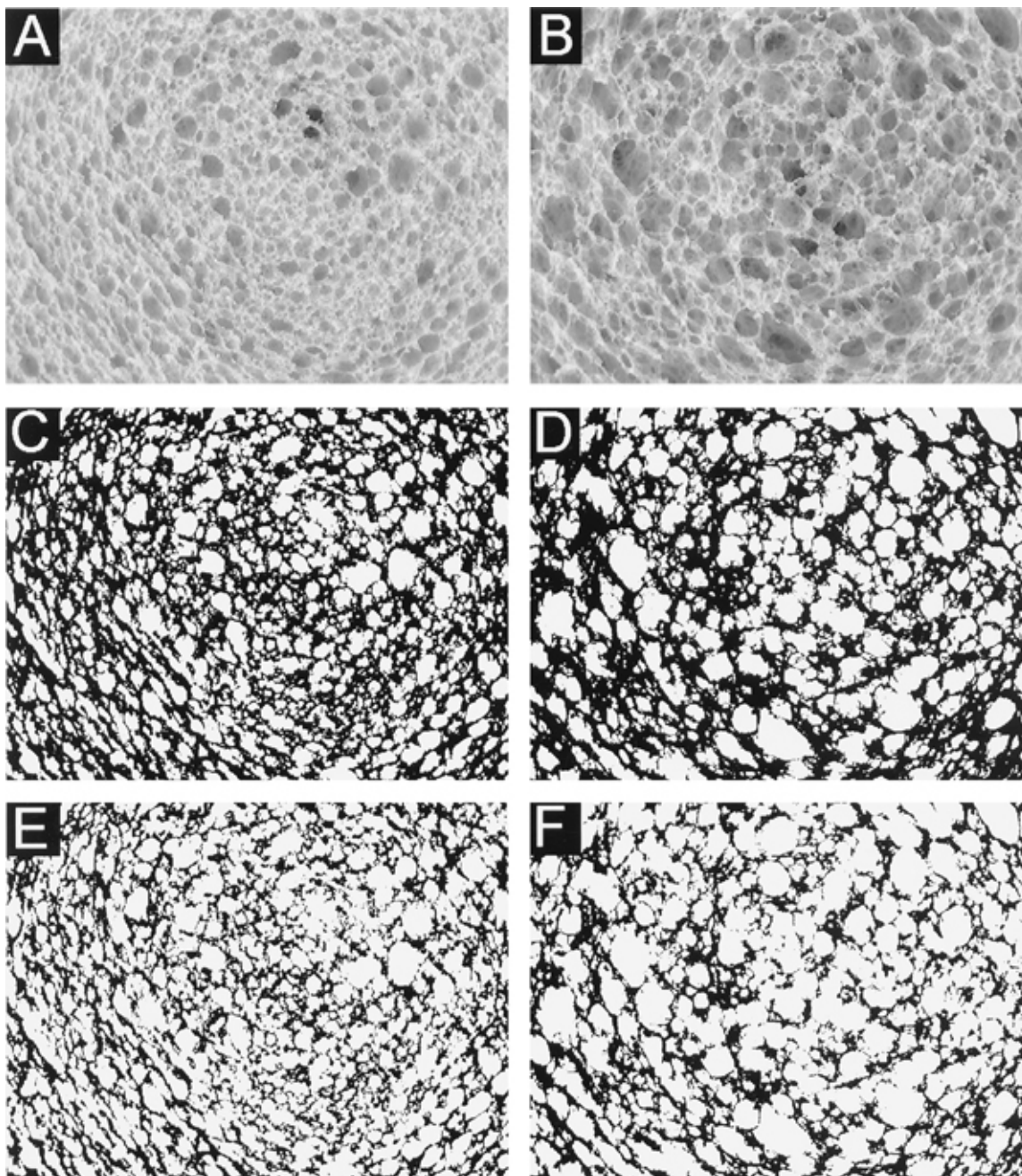


**Fig. 1.** Original (A and B) and processed digital images showing computed cells (C and D) and cell wall structures (E and F) of typical slices of under- and overproofed CWRS bread, respectively.

were acquired against a black cardboard background. Subsequently, crumb specimens were placed into covered petri dishes for the drying experiment. The crumb grain parameters were automatically determined as previously reported (Sapirstein et al 1994): crumb brightness, CWT, mean cell area, crumb fineness (measured as the number of cells/cm<sup>2</sup>), and void fraction (VF), which measures the proportion of the cross-sectional area of the crumb FOV containing gas cells. The VF signified the ratio of cell to total area.

### Drying

Once all the fresh crumb specimens were imaged, they were exposed to ambient temperature and humidity conditions for three drying periods to achieve ≈8% moisture loss each time. The drying times, determined from preliminary experiments, were 30, 70, and 130 min; increasing times were required because the bread tended to lose moisture at a slower rate after each drying treatment. Specimens were inverted at the midpoint of each drying period to minimize physical distortion of the crumb pieces and achieve uniform moisture loss. At the end of each drying period, the samples were kept in covered petri plates for 2 hr to permit moisture equilibration. The density and crumb grain of the specimens were then determined as for the fresh specimens.

### Statistical Analysis

Data were analyzed by statistical software (SAS Institute Inc., Cary, NC). Computed crumb grain features taken from opposite sides of each specimen were averaged. Correlation analysis between crumb density and each crumb grain feature was computed. Stepwise linear regression analysis was used to determine the model for estimation of bread crumb density. Analysis of variance (ANOVA) for various processing conditions was performed using the general linear models (GLM) procedure. Differences between dough mixing and proofing times were compared using Duncan's multiple range test.

TABLE I  
Loaf Volume (cm<sup>3</sup>) as a Function of Mixing and Proof Time<sup>a</sup>

Proof Time (min)	Dough Mixing Time Relative to Optimum				
	-40%	-20%	Optimum	+20%	+40%
CWRS					
35	596d	660ab	666a	650bc	643c
70	826c	936ab	958a	933b	926b
105	1,030c	1,146a	1,166a	1,106b	1,076b
CPS					
35	556c	600a	610a	600a	580b
70	780d	830b	902a	836ab	806c
105	957c	1,106a	1,040b	1,060b	1,060b

<sup>a</sup> Statistical analysis was performed separately for each type of flour. Means with different letters across each row are significantly different ( $P < 0.05$ ). Means in each column are significantly different ( $P < 0.05$ ).

TABLE II  
Crumb Density (g/cm<sup>3</sup>) as a Function of Dough Mixing and Proof Time<sup>a</sup>

Proof Time (min)	Dough Mixing Time Relative to Optimum				
	-40%	-20%	Optimum	+20%	+40%
CWRS					
35	0.215a	0.190bc	0.190c	0.196bc	0.197b
70	0.142a	0.132b	0.131b	0.129b	0.129b
105	0.111a	0.108ab	0.101c	0.105bc	0.103c
CPS					
35	0.233a	0.215b	0.213b	0.209b	0.216b
70	0.145a	0.141a	0.145a	0.143a	0.142a
105	0.120a	0.107bc	0.108b	0.103c	0.103c

<sup>a</sup> Statistical analysis was performed separately for each type of flour. Means with different letters across each row are significantly different ( $P < 0.05$ ). Means in each column are significantly different ( $P < 0.05$ ).

### Baking Results

Loaf volume and crumb density as functions of dough mixing and proofing times are shown in Tables I and II. Loaf volume ranges were 570–1,260 cm<sup>3</sup> and 540–1150 cm<sup>3</sup> for the CWRS and CPS bread, respectively. Crumb density ranges were 0.09–0.248 g/cm<sup>3</sup> and 0.088–0.252 g/cm<sup>3</sup> for the CWRS and CPS bread, respectively. These values are substantially lower than densities of bread (based on loaf volume and weight) reported by Whitworth and Alava (1999) for optimally processed bread mixed on different mixers. The lower crumb density obtained in this study likely arises as a result of selecting relatively small crumb sections located centrally in the loaf where bread density appears to be lower (Ponte et al 1962, Short and Roberts 1971).

Dough mixing and proofing times significantly ( $P < 0.05$ ) affected loaf volume (Table I) and crumb density (Table II) of CWRS. Similar results were obtained for CPS bread, except for optimum proofing (70 min), where dough mixing time had no significant effect on the mean density of bread crumb (Table II,  $P = 0.38$ ). Varying proofing time had a more pronounced effect on loaf volume and bread crumb density than variation in dough mixing time. Altering the proofing time resulted in significant differences in loaf volume and crumb density ( $P < 0.05$ ) for all dough mixing times and for both types of flours. This experiment also showed that there was a strong negative correlation between loaf volume and bread crumb density ( $r = -0.96$ ) for both types of flours. The strength of this result is important because by predicting or determining the density, one can accurately estimate loaf volume.

### Effects of Dough Proofing on Crumb Grain

Both dough mixing and proofing have major effects on bread quality, including crumb grain (Kamman 1970). The purpose of the final proof is to allow the dough after panning to regain an extensible character and a high level of aeration to subsequently yield a loaf with a desired volume and crumb grain (Pyler 1988). As expected, different dough proofing times had a significant effect on the crumb grain of CWRS and CPS bread (Table III).

Compared to 70-min (optimum) proof time, the 35-min proof time of CWRS dough resulted in bread crumb with a 3% brighter crumb, 10% smaller cells, 18% more cells/cm<sup>2</sup>, 5.5% lower VF, and 6.4% thinner cell walls. For CPS bread crumb, the effect of underproofing on crumb grain features was larger on average. The

TABLE III  
Effect of Proof Time on Crumb Grain of Bread Prepared Using Optimally Mixed Dough<sup>a</sup>

Grain Features	Proof Time (min)		
	35	70 (optimum)	105
CWRS			
Average gray level	175.0a	168.8b	158.0c
Void fraction	0.4852c	0.5132b	0.5157a
Number of cells/cm <sup>2</sup>	113a	96b	80c
Average cell size (mm)	0.712c	0.795b	0.885a
Average cell area (mm <sup>2</sup> )	0.400c	0.500b	0.622a
Median cell area (mm <sup>2</sup> )	0.033b	0.034b	0.041a
CWT (mm)	0.647c	0.792b	0.813a
CPS			
Average gray level	177.4a	166.3b	158.2c
Void fraction	0.4741c	0.4974b	0.5163a
Number of cells/cm <sup>2</sup>	103a	77b	64c
Average cell size (mm)	0.725c	0.888b	0.967a
Average cell area (mm <sup>2</sup> )	0.419c	0.623b	0.738a
Median cell area (mm <sup>2</sup> )	0.040b	0.048a	0.051a
CWT (mm)	0.736c	0.828b	0.895a

<sup>a</sup> Statistical analysis was performed separately for each type of flour. Means with different letters across each row are significantly different ( $P < 0.05$ ). CWT = cell wall thickness.

35-min proof time of CPS dough resulted in 6.3% brighter crumb, 18.4% smaller cell size, 34% more cells/cm<sup>2</sup>, 4.6% lower VF, and 11% thinner cell walls. The effects of underproofing on crumb grain as determined by DIA, were consistent with observations made by Kamman (1970), except for CWT, where he observed thicker cell walls for underproofed bread. The results of this study indicated that, upon increasing proofing time from 35 to 70 min, a greater degree of gas cell coalescence had occurred for the CPS dough than for the CWRS dough, resulting in a coarser crumb grain (Baker 1941). This result is consistent with the relative strengths of the two flours; CPS dough was weaker with ≈34% lower dough mixing requirements.

For both types of flour, extending the proofing time to 105 min resulted in lower crumb brightness, larger cells, higher VF, coarser crumb (fewer cells/cm<sup>2</sup>), and thicker cell walls when compared with optimally proofed samples. These results were also attributed to greater degree of gas cell coalescence as proofing time was increased. The effect of increasing proof time on increasing average CWT was interesting because it appears to run counter to expectations; that is, it is plausible that gas cell coalescence during overextended proofing could result in larger cells on average (as was found) with thinner cell walls (which was not seen). To more fully explore the nature of this result, careful examination of all the digital images of bread crumb grain was performed, as well as their corresponding images segmented by the *K*-means algorithm into three partitions (Sapirstein et al 1994). Use of three partitions permits isolation of cell wall structures in the images, hence reducing the complexity of the crumb grain. A clear distinction in cell wall structure between under- and overproofed bread was revealed that supports the computed results for CWT (Table III). A typical result is shown in Fig. 1E and F for isolated cell walls of under- and overproofed bread, respectively. In accordance with Gibson and Ashby (1997), the structure of cellular solids can be classified into cell faces and cell edges (vertices where cell faces meet). For the underproofed slice (Fig. 1E), it is clear that the cell walls comprising both cell faces and edges are distributed much more evenly than that for overproofed bread. By comparison, overproofed bread (Fig. 1F) has noticeably thicker cell edges and a much less uniform CWT distribution than does underproofed bread. Accordingly, it is possible that this would contribute to larger CWT values, on average, for overproofed bread. While overproofed bread may have thinner cell faces than underproofed bread, the perception that overproofed bread has relatively thinner cell walls on average when compared with that of underproofed bread may not be correct.

### Effects of Dough Mixing on Crumb Grain

Dough mixing is an important process that significantly affects the baking process and, consequently, the quality of the bread. Mixing has many functions; it serves to incorporate various ingredients into a dough mass, occlude air, and develop the gluten. The effects of dough mixing time on crumb grain of optimally proofed CWRS and CPS bread are shown in Table IV. Our expectation was that mixing to optimum would produce bread with the finest grain and brightest crumb. Results indicated that this expectation was met only for the CWRS bread.

CWRS dough undermixed by 40% resulted in bread crumb with very poor grain (coarser) characteristics that were significantly different from those of optimally mixed dough. The crumb of the 40% undermixed dough had lower crumb brightness, fewer cells/cm<sup>2</sup>, thicker cell walls, and larger gas cells when compared with optimally mixed dough (Table IV). These objectively determined results by DIA were similar to those observed by Kamman (1970), who reported that undermixed dough produced a crumb with thick cell walls, large cells, and a dull color. The effect of undermixing is believed to be due to the failure of the dough to exhibit good sheet-forming and gas retention properties (Tipples and Kilborn 1974).

Overmixing dough made from CWRS flour by 40% had significant effects on both VF and CWT. No effects were observed for the other crumb grain features. The changes in crumb character as a result of overmixing are presumably due to the disruption of the continuous membrane structure of gluten in an optimally mixed dough (Paredes-Lopez and Bushuk 1983). It was noteworthy that the DIA results confirmed what is generally known about under- and overmixing doughs: that undermixing produces the larger negative effect (Tipples and Kilborn 1974). Optimally mixed dough yielded crumb with the highest degree of brightness, thinnest cell walls, smallest average area, and highest number of cells per unit area. The higher crumb brightness of optimally mixed CWRS dough can be partly attributed to the finer cellular structure of the bread and to the shiny appearance of the thin film of gluten lining the surface of the cell (Baker 1941).

It was unclear why the CPS bread did not show any consistent trend related to dough mixing treatments, as was observed for the CWRS bread. It should be noted that the CPS flour, and CPS wheat in general, was not optimally suited for breadmaking because of its intrinsically lower protein content and protein quality, as reflected in its lower absorption and weaker dough mixing properties. Presumably, the equivocal response of this flour to varying dough mixing conditions in the short-time test baking process

TABLE IV  
Effect of Mixing on Crumb Grain of Bread Prepared Using Optimally Proofed Dough<sup>a</sup>

Grain Features	Dough Mixing Time Relative to Optimum				
	-40%	-20%	Optimum	+20%	+40%
<b>CWRS</b>					
Average gray level	163.7b	167.9a	168.8a	169.3a	169.1a
Void fraction	0.4980b	0.5014b	0.5132a	0.4986b	0.4963b
Number of cells/cm <sup>2</sup>	82b	95a	96a	88ab	93a
Average cell size (mm)	0.864a	0.797b	0.795b	0.824ab	0.803b
Average cell area (mm <sup>2</sup> )	0.595a	0.505b	0.500b	0.539ab	0.509b
Median cell area (mm <sup>2</sup> )	0.045a	0.040ab	0.034b	0.046a	0.041ab
CWT (mm)	0.847a	0.736bc	0.692c	0.751b	0.749b
<b>CPS</b>					
Average gray level	165.1c	169.0b	166.3c	170.4a	165.8c
Void fraction	0.5034a	0.5033a	0.4974a	0.5017a	0.5022a
Number of cells/cm <sup>2</sup>	76c	89a	77c	79bc	83ab
Average cell size (mm)	0.897a	0.806b	0.888a	0.872a	0.837b
Average cell area (mm <sup>2</sup> )	0.637a	0.514c	0.623a	0.600ab	0.553bc
Median cell area (mm <sup>2</sup> )	0.0395b	0.0394b	0.0477a	0.04927a	0.0395b
CWT (mm)	0.828a	0.772b	0.828a	0.776b	0.803ab

<sup>a</sup> Statistical analysis was performed separately for each type of flour. Means with different letters across each row are significantly different ( $P < 0.05$ ). CWT = cell wall thickness.

ture that was used reflects this intrinsic difference in the protein component of the CPS flour when compared with the CWRS counterpart.

### Relationship Between Crumb Density and Crumb Grain

The response of computed crumb grain features in the experiments described above were examined for their relationships to crumb density (Table V). Correlation analysis showed that crumb brightness (or average GL) was the grain characteristic most strongly related to crumb density. This was expected because bread crumb with higher density had a finer structure, or a larger number of cells per unit area with a smaller average cell size, resulting in greater reflectance into the imaging system. Sapirstein et al (1994) also observed that oxidant formula bread crumb, with a higher average GL than control formula bread, had a larger number of cells and smaller mean cell area. All these results are in agreement with the observation of Burhans and Clapp (1942), who found that the whiteness in bread crumb was enhanced by the presence of a large number of small cells.

The computed VF of crumb also had a relatively high (negative) correlation with crumb density. The VF value ranges were 0.438–0.539% for CWRS and 0.443–0.534% for CPS bread crumb. On the expectation that surface density is an accurate representation of volume density (Underwood 1970), the VF was expected to yield the best estimate of density because  $1-VF$  represents the surface density (the ratio of the area of all cell wall material to the area of the FOV). However, this was not the case. It is evident that VF values have been significantly underestimated based on the difference between typical volumes of baked bread ( $950 \text{ cm}^3$ ) and typical volumes of the corresponding degassed dough cylinders after sheeting ( $200 \text{ cm}^3$ ); the VF in this case should be 0.79.

There are at least two possible explanations for underestimating the VF values. First, there are intramural cells or pockets surrounding the larger cells in cell walls (Burhans and Clapp 1942). These intramural cells could not be detected by the DIA system because of the limiting spatial resolution of the system; the smallest cells that were detected are  $70 \mu\text{m}$  in diameter. Although these cells are small in size, they could be present in large numbers (Campbell et al 1991). In fact, it was previously observed (Sapirstein et al 1994) by DIA that the largest fraction of cells in bread crumb were those of smallest size. Therefore, not being able to detect cells smaller

than the limiting resolution of the DIA system can result in an underestimation of the VF value. This limitation could be overcome by increasing the resolution of the DIA system.

The second reason for the lower VF values is that, on average, the gas cell size observed by DIA at the surface of the bread slice is lower than the actual cell size (see Appendix A). Assuming that gas cells are spherical in shape and slicing is random, the cell size observed at the surface is always smaller than the actual diameter of the cell because of the impossibility that all cells are precisely bisected when bread is sliced. This view was previously expressed (Sapirstein et al 1994) for a related concept in regard to the accuracy of CWT computation by the DIA system. It was observed that the two-dimensional image analysis approach used in that (and the present) study most probably overestimates the actual CWT in uncut bread. The overestimation derives from the likelihood that only a small proportion of neighboring crumb cells, exposed on the cut surface of a slice of bread, are actually bisected. Therefore, to correct for this underestimation of the VF, the average area of gas cell and VF values must be multiplied by a factor of 1.5 (Appendix A). If VF values are to be used as a means of estimating the density of the slice, then they must be multiplied by a factor of 1.7. This is because, on average, cell volume based on cell size observations of the surface of the slice is 41% lower than the actual cell volume, assuming that cells are spherical in shape and sectioned randomly to give cells with a uniform size distribution. The mathematical explanation of this interpretation is presented in Appendix B.

Compared to crumb brightness and the VF, the remaining crumb grain parameters, including number of cells/ $\text{cm}^2$ , average cell size, average cell area, CWT, and median cell size were correlated with crumb density to a lesser extent in the range 0.58–0.73 (Table V).

### Model for Prediction of Bread Crumb Density

Despite the relatively high correlations between average GL and the VF to crumb density, these two parameters could account for no more than 50–70% of the variation in crumb density, depending on bread type. To establish a more robust estimate of crumb density, a combination of two or more crumb grain features was considered and evaluated. Stepwise linear regression analysis indicated that a two-variable model comprising the VF and CWT was the best two-variable model (yielding the highest  $R^2$ ) for predicting bread crumb density of fresh bread samples. This model (VF and CWT) also provided a plausible and relatively simple representation of bread crumb structure. In addition, models with more than two variables did not yield significantly higher  $R^2$  values for predicting crumb density. The two-variable multiple correlation coefficients for prediction of CWRS and CPS bread crumb densities by DIA of crumb grain were  $r = 0.90$  and  $0.92$ , respectively. The pertinent linear regression equations were:

$$\text{Density} = 1.05 - (1.52 \times \text{VF}) - (2.04 \times \text{CWT}) \quad (1)$$

for CWRS ( $P < 0.0001$ )

$$\text{Density} = 1.12 - (1.67 \times \text{VF}) - (1.59 \times \text{CWT}) \quad (2)$$

for CPS ( $P < 0.0001$ )

where density is expressed in  $\text{g/cm}^3$ , CWT in cm, and the coefficients have units of  $\text{g/cm}^3$ , except for the CWT coefficient which has units of  $\text{g/cm}^4$ .

To evaluate the predictive capacity of these equations for determining density from image analysis of bread crumb, Equation 1, which had been developed from images of CWRS bread crumb, was tested on images of CPS bread crumb. A good fit ( $r = 0.90$ ) was obtained. Similarly, using Equation 2 on the CWRS bread crumb images gave  $r = 0.89$ . Therefore, based on this result and on the similarity in image parameters and coefficients in Equations 1 and 2, stepwise linear regression analysis was used to develop an

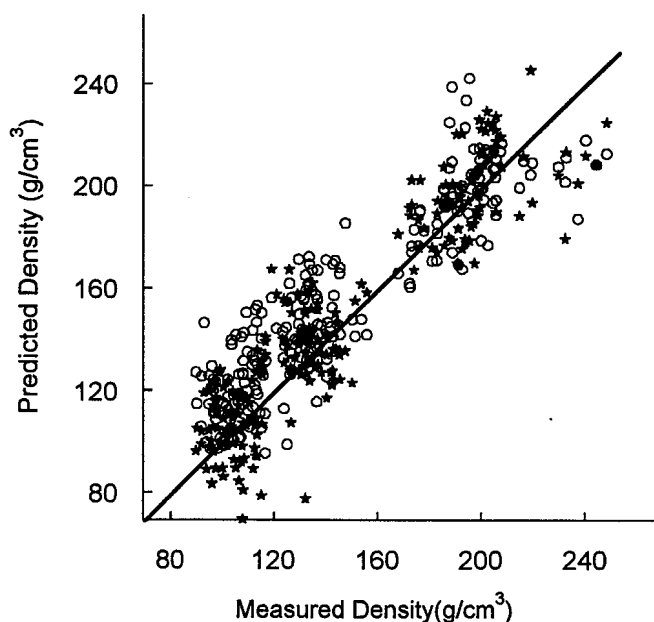


Fig. 2. Relationship between measured and predicted density of CWRS (○) and CPS (★) bread using Equation 3.

equation from both flour types. Again, it indicated that the same two crumb grain parameters (VF and CWT) were the best two-variable model for crumb density prediction:

$$\text{Density} = 1.08 - (1.62 \times \text{VF}) - (1.59 \times \text{CWT}) \quad (3)$$

$(P < 0.0001)$

The relationship between measured and predicted density of crumb using Equation 3 for the two types of bread is shown in Fig. 2. The multiple correlation coefficient for the combined data model ( $r = 0.89$ ) was comparable to that obtained for CWRS or CPS bread individually.

In all three density prediction equations, the VF had a negative partial correlation coefficient because surface density (1-VF) is positively correlated with crumb density. The rationale for CWT as a predictor of crumb density is straightforward: it represents the quantity of material surrounding the gas cells, whose density appears to vary with processing conditions such as dough mixing and proofing rather than being constant. Variation in cell wall density has been reported for extruded cereal products (Donald 1994, and references therein). In addition, it is conceivable that CWT may account for

**TABLE V**  
Correlation Coefficients Between Crumb Grain Parameters and Crumb Density

Grain Feature	Correlation Coefficients	
	CWRS	CPS
Average gray level	0.77	0.84
Void fraction	-0.71	-0.82
Number of cells/cm <sup>2</sup>	0.70	0.73
Average cell size (mm)	-0.68	-0.69
Average cell area (mm <sup>2</sup> )	-0.65	-0.68
Cell wall thickness (mm)	-0.58	-0.59

**TABLE VI**  
Correlation Coefficients for Measured and Predicted Density of Dried Bread Crumb Using a Two-Variable Linear Regression Model<sup>a</sup>

Drying Time (min)	Flour Type	
	CWRS	CPS
0	0.91	0.92
30	0.89	0.90
70	0.91	0.91
130	0.88	0.91

<sup>a</sup> Equation 3.

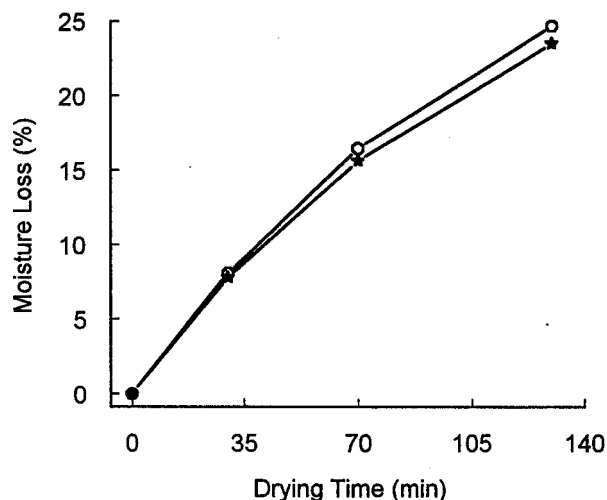


**Fig. 3.** Percentage moisture loss of CWRS (○) and CPS (★) bread crumb as a function of drying time.

the undetected intramural cells which, as mentioned above, are located in the cell walls (Burhans and Clapp 1942), and that these may vary with processing conditions. Therefore, these results clearly indicate that the DIA approach used in this study can accurately predict bread crumb density based on crumb grain structure.

### Effect of Drying on Density and Grain of Bread Crumb

To further assess the ability of image analysis to predict bread density, Equation 3 was tested on bread samples with densities altered as a result of drying. The percentage moisture loss from bread crumb as a function of drying time is shown in Fig. 3. After each drying period the moisture loss was ≈8%. Although the rate of moisture loss was approximately constant for both types of flours, the change in bread crumb density with increasing drying time appeared to be different. For CPS bread, the change in crumb density as a function of drying time was linear ( $r = 0.97$ ), whereas for CWRS bread, crumb density increased rapidly during the first 30 min (first drying period) and then leveled off (Fig. 4). The initial rapid increase in density of CWRS bread crumb was due to a larger reduction in the volume of the specimen because the crumb was soft and deformed easily in the early stage of drying (Steller and Bailey 1938). For other drying times, the change in CWRS crumb specimen volume was almost equal to the change in weight as the crumb structure became more rigid and resistant to shrinking. This effect may arise as a result of a relatively more continuous protein-starch matrix in the dough contributed by the higher protein content of the CWRS flour (Paredes-Lopez and Bushuk 1983), which caused a relatively slower decrease in volume upon further drying. The lower protein content of CPS bread that resulted in a weaker crumb structure permitted a constant shrinkage of specimens as they were subjected to drying.

Because the volume of bread crumb decreases as moisture is lost, it can be assumed that drying is accompanied by changes in crumb structure. Because the density of bread crumb made from the CWRS and CPS flours changed in different ways, the change in structure was also expected to be different. Upon drying, it was expected that cell size, VF, and CWT would decrease, and that crumb brightness and the number of cells/cm<sup>2</sup> would increase.

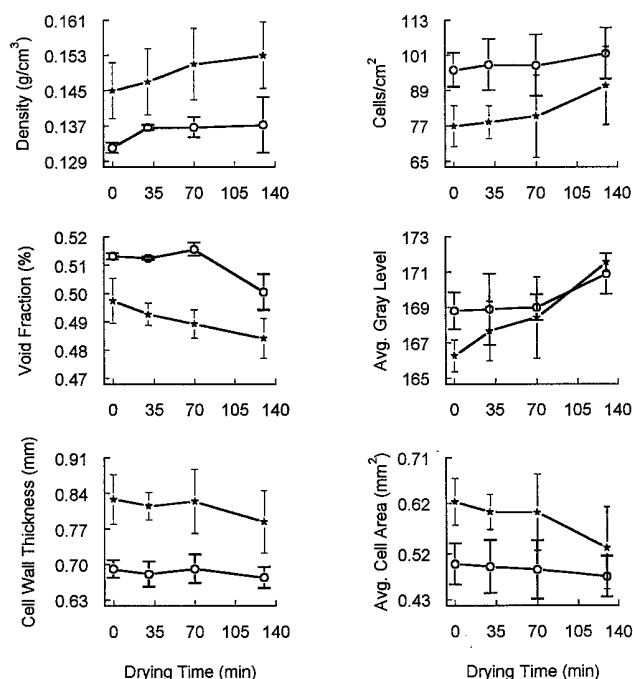


**Fig. 4.** Effect of drying time on density, void fraction, cell wall thickness, cells/cm<sup>2</sup>, average gray level, and average cell area of optimally baked CWRS (○) and CPS (★) bread.

These expected effects were observed in the structure of the drying crumb as measured by DIA (Fig. 4).

Regression analysis for measured density and grain features of dried bread samples was also performed. The same two variables, VF and CWT, were highly correlated with crumb density. For the various drying times, the multiple correlation coefficients were  $r = 0.88-0.91$  and  $r = 0.90-0.92$  for CWRS and CPS bread, respectively. If the regression model (Eq. 3) for crumb density prediction by image analysis is robust, then changes in density that result from drying of the bread crumb should also be accurately predicted by the same model. Multiple correlation coefficients (Table VI) for the relationship between measured and predicted crumb density for dried bread crumb confirmed that DIA prediction of density by Equation 3 was robust enough that the density of dried bread could also be accurately predicted on the basis of crumb structure.

## CONCLUSIONS

In this study, the relationship between bread crumb density and bread crumb grain was assessed to test the validity and accuracy of a digital imaging system for direct determination of crumb grain parameters. Using two widely different flour types, various dough mixing and proofing times were used to create a range of loaf volumes and corresponding bread crumb densities. Compared to dough mixing, varying proofing time had a more pronounced effect on crumb density and crumb grain parameters for both flours. Average gray level and VF of crumb were most strongly correlated with crumb density. A two-variable model using VF and CWT permitted very good prediction of the density of fresh and dried bread crumb samples. This result indicates successful validation of the imaging system to accurately measure crumb grain features. Therefore, the assessment of the relationship between structure and textural properties in bread crumb by DIA would seem feasible.

## ACKNOWLEDGMENTS

We gratefully acknowledge the financial support of the Natural Sciences and Engineering Research Council of Canada. We thank Randy Roller for assistance with the image analysis system and statistical analysis. We also thank the Canadian International Grains Institute for the flour samples used in this study.

## LITERATURE CITED

- Attenburrow, G. E., Goodband, R. M., Taylor, L. J., and Lillford, P. J. 1989. Structure, mechanics and texture of a food sponge. *J. Cereal Sci.* 9:61-70.
- Baker, J. C. 1941. The structure of the gas cell in bread dough. *Cereal Chem.* 18:34-41.
- Barrett, A. H., Cardello, A. V., Leshner, L. L., and Taub, I. A. 1994. Cellularity, mechanical failure, and textural perception of corn meal extrudates. *J. Texture Stud.* 25:77-95.
- Bertrand, D., Le Guerneve, C., Marion, D., Devaux, M. F., and Robert, P. 1992. Description of the textural appearance of bread crumb by video image analysis. *Cereal Chem.* 69:257-261.
- Bhatnagar, S., and Hanna, M. A. 1997. Modification of microstructure of starch extruded with selected lipids. *Starch/Staerke* 49:12-20.
- Burhans, M. E., and Clapp, J. 1942. A microscopic study of bread and dough. *Cereal Chem.* 19:196-216.
- Campbell, G. M., Rielly, C. D., Fryer, P. J., and Sadd, P. A. 1991. The measurement of bubble size distribution in an opaque food fluid. *Trans. Inst. Chem. Eng. Part C* 69:67-76.
- Chan, J. P., and Batchelor, B. G. 1993. Machine vision for the food industry. Pages 58-101 in: *Food Process Monitoring Systems*. A. C. Pinder and G. Godfrey, ed. Chapman and Hall: London.
- Donald, A. M. 1994. Physics of foodstuffs. *Rep. Prog. Phys.* 57:1081-1135.
- Gerrard, D. E., Gao, X., and Tan, J. 1996. Beef marbling and color score determination by image processing. *J. Food Sci.* 61:145-148.
- Gibson, L., and Ashby, M. F. 1988. *Cellular Solids*. Pergamon Press: Oxford.
- Gibson, L. J., and Ashby, M. F. 1997. The structure of cellular solids. Pages 15-51 in: *Cellular Solids*. 2nd ed. Cambridge University Press: Cambridge.
- Gunasekaran, S., and Ding, K. X. 1994. Using computer vision for food quality evaluation. *Food Technol.* 48(6):151-154.
- Hlynka, I., and Anderson, J. A. 1965. Laboratory dough mixer with an air-tight bowl. *Cereal Chem.* 32:83-87.
- Kamman, P. W. 1970. Factors affecting the grain and texture of white bread. *Baker's Dig.* 44(2):34-38.
- Kilborn, R. H., and Dempster, C. J. 1965. Power-input meter for laboratory dough mixer. *Cereal Chem.* 42:432-435.
- Kilborn, R. H., and Tipples, K. H. 1981. Canadian test baking procedure. II. GRL-Chorleywood method. *Cereal Foods World* 26:628-630.
- Paredes-Lopez, O., and Bushuk, W. 1983. Development and "undevelopment" of wheat dough by mixing: Microscopic structure and its relations to breadmaking quality. *Cereal Chem.* 60:24-27.
- Ponte, J. G., Titcomb, S. T., and Cotton, R. H. 1962. Flour as a factor in bread firming. *Cereal Chem.* 39:437-444.
- Pyler, E. J. 1988. *Baking Science and Technology*. Sosland Publishing Co: Merriam, KS.
- Rogers, D., Day, D. D., and Olewnik, M. C. 1995. Development of an objective crumb-grain measurement. *Cereal Foods World* 40:498-501.
- Sapirstein, H. D. 1995. Quality control in commercial baking: Machine vision inspection of crumb grain in bread and cake products. Pages 23-33 in: *Proceedings of the Food Processing Automation Conference, IV*. ASAE: St. Joseph, MI.
- Sapirstein, H. D. 1999. The imaging and measurement of bubbles in bread. Pages 233-243 in: *Bubbles in Food*. G. M. Campbell, C. Webb, S. S. Pandiella, and K. Niranjana, eds. Am. Assoc. Cereal Chem.: St. Paul, MN.
- Sapirstein, H. D., Inoue, Y., and Bushuk, W. 1992. Instrumental measurement of bread crumb grain features by digital image analysis. *Cereal Foods World* 37:552-553.
- Sapirstein, H. D., Roller, R., and Bushuk, W. 1994. Instrumental measurement of bread crumb grain by digital image analysis. *Cereal Chem.* 71:383-391.
- Short, A. L., and Roberts, E. A. 1971. Pattern of firmness within a bread loaf. *J. Sci. Food Agric.* 22:470-472.
- Steller, W. R., and Bailey, C. H. 1938. The relation of flour strength, soy flour and temperature of storage to the staling of bread. *Cereal Chem.* 15:391-401.
- Tao, Y., Heinemann, P. H., Varghese, Z., Morrow, C. T., and Sommer, H. J. 1995. Machine vision for color inspection of potatoes and apples. *Trans. ASAE* 38:1555-1561.
- Tipples, K. H., and Kilborn, R. H. 1974. Dough development for short breadmaking processes. *Baker's Dig.* 48(5):34-39.
- Underwood, E. E. 1970. *Quantitative Stereology*. Addison-Wesley Publishing Co.: Reading, MA.
- Wang, I., and Coles, G. D. 1993. Image processing methods for determining bread texture. Pages 125-132 in: *Proc. New Zealand Conference on Image and Vision Computing, 1st. Industrial Research Ltd.*: Auckland.
- Wang, I., and Coles, G. D. 1994. Objective measurement of bread crumb texture. *Optics in Agriculture, Forestry, and Biological Processing. Proc. SPIE* 2345:85-91.
- Whitworth, M. B., and Alava J. M. 1999. The imaging and measurement of bubbles in bread doughs. Pages 221-231 in: *Bubbles in Food*. G. M. Campbell, C. Webb, S. S. Pandiella, and K. Niranjana, eds. Am. Assoc. Cereal Chem.: St. Paul, MN.
- Yamada, Y., and Preston, K. R. 1992. Effects of individual oxidants on oven rise and bread properties of Canadian short process bread. *J. Cereal Sci.* 15:237-251.
- Zayas, I. Y. 1993. Digital image texture analysis for bread crumb grain evaluation. *Cereal Foods World* 38:760-766.
- Zayas, I. Y., Chung, O. K., and Caley, M. S. 1995. Neural network classification and machine vision for bread crumb grain evaluation. *Machine vision applications, architectures, and systems integration. Proc. SPIE* 2597:292-309.

[Received February 1, 1999. Accepted June 22, 1999.]

## APPENDIX A

The cell area obtained by a digital image analysis (DIA) system on the basis of the examined surface of bread crumb is underestimated. Regardless of whether a given gas cell (spherical shape) is sectioned below or above its center, the resulting cross-sectional area is smaller than the cross-sectional area passing through the center (center of sphere). Therefore, in order to determine the degree of underestimation, the average of all possible cross-sectional areas passing through the gas cell should be computed and compared with the cross-sectional area that passes through the center.

*Assumption 1.* Gas cells have a uniform size distribution and are spherical in shape with a radius  $R$  giving a circular cell of radius  $r$  at the surface of the bread slice (Fig. A1) where  $r = (R^2 - x^2)^{1/2}$ ;  $x$  = distance from the center of the spherical cell to the surface of the slice, with  $-R \leq x \leq R$ .

*Assumption 2.* During bread slicing, the spherical cells are randomly sectioned at a distance  $x$  from their centers.

*Assumption 3.* The sectioned cells are representative of the population of cells in a given slice because the number of cells observed at the surface of a bread slice was 1,017–3,850.

The average gas cell area of radius  $r$ , sectioned at a distance  $x$  from the center plane is described by the function  $A_{ave}(x)$ :

$$A_{ave}(x) = \frac{1}{2R} \int_{-R}^R \pi(R^2 - x^2) dx$$

$$A_{ave}(x) = \frac{2}{3} \pi R^2$$

Therefore, on average, the cell area observed at the surface of the bread slice represents 66% of the cross-sectional area at the center of the sphere.

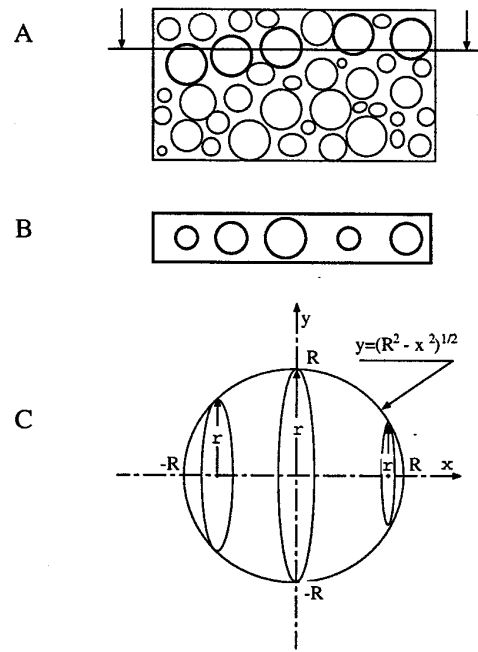


**Fig. A1.** Schematic representation of bread structure (A) sectioned as indicated with arrows, cross-sectional area of sectioned cells (B), and model of individual cell sectioned at three different locations, producing different radii  $r$  (C). The equation calculates the radius  $r$  as a function of  $x$ , distance from the center of the sphere, and the radius ( $R$ ) of the sphere itself.

## APPENDIX B

Depending on whether the spherical (assumed) gas cells of radius  $R$  are sectioned above or below their centers, the exposed cell volume based on cell size observed at the surface of the bread slice could be under- or overestimated (Fig. B1). This problem arises from the two-dimensional nature of the digital image analysis (DIA) system which computes the cell radius as  $(\text{Area}/\pi)^{1/2}$  based on cell area observed at the cut surface. Consequently, the exposed cell volume  $V_E(x)$  derived from the DIA system is equivalent to  $2/3\pi r^3$ , where  $r = (R^2 - x^2)^{1/2}$  and  $-R \leq x \leq R$  (see Fig. B1). In contrast, the true cell volume  $V_T(x)$  corresponds to the portion of the gas cell below the sectioning plane. Therefore, to determine whether, on average, the gas cell volume is properly estimated, one needs to compare the mean exposed cell volume  $V_{Eave}(x)$  and the mean true cell volume  $V_{Tave}(x)$ , for all possibilities of sectioning a gas cell. The equation  $V_T(x)$  of true cell volume, the portion of the cell below the sectioning plane, as a function of distance  $x$  from the center can be determined by the volumes of revolution theorem.

This equation is derived as:

$$V_T(x) = \int \pi(R^2 - x^2) dx$$

For simplification,  $R = 1$ , so  $-1 \leq x \leq 1$ . Therefore:

$$V_T(x) = \int \pi(1 - x^2) dx$$

$$V_T(x) = \pi \left( x - \frac{x^3}{3} + \frac{2}{3} \right)$$

Considering all sectioning possibilities where  $-1 \leq x \leq 1$ ,  $V_{Tave}(x)$  is:

$$V_{Tave}(x) = \frac{1}{2} \int_{-1}^1 \pi \left( x - \frac{x^3}{3} + \frac{2}{3} \right) dx$$

$$V_{Tave}(x) = \frac{2}{3} \pi$$

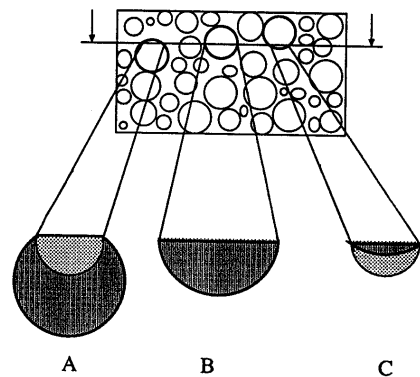


**Fig. B1.** Schematic diagram of a section of bread crumb and actual and predicted volumes of three gas cells cut at different distances from the center. Cell A cut above center, cell B cut in center, and cell C cut below center. For cells A and C, the digital imaging system would under- and overestimate, respectively, the void fraction as indicated by the ratio of darker to lighter regions.

In contrast, by DIA,  $V_{Eave}(x)$ , based on cell size at the sample surface where  $-1 \leq x \leq 1$ , is:

$$V_{Eave}(x) = \frac{I}{2} \int_{-1}^1 V_o(x) dx$$

$$V_{Eave}(x) = \frac{I}{2} \int_{-1}^1 \frac{2}{3} \pi (1 - x^2)^{3/2} dx$$

Let  $x = \sin\theta$ , so  $d\theta = \cos\theta d\theta$ , so that  $-\frac{\pi}{2} \leq \theta \leq \frac{\pi}{2}$

$$V_{Eave}(x) = \frac{I}{3} \pi \int_{-\pi/2}^{\pi/2} (\cos\theta)^4 d\theta$$

$$V_{Eave}(x) = \frac{I}{3} \pi \int_{-\pi/2}^{\pi/2} \left[ \frac{3}{8} + \frac{1}{2} \cos 2\theta + \frac{1}{8} \cos 4\theta \right] d\theta$$

$$V_{Eave}(x) = \frac{I}{8} \pi^2$$

By comparing  $V_{Tave}(x)$  and  $V_{Eave}(x)$ , one can conclude that by estimating the cell volume from surface measurements, the volume of the cells is underestimated by a factor of 1.70.